

Figure 1 | The trajectory of New Horizons through the solar system. Data collection periods of relevance to this study are indicated. Both the $x - y$ and $r - z$ planes are shown (**a, b**, respectively), with the axes in solar ecliptic units and $d_r = \sqrt{d_x^2 + d_y^2}$. New Horizons was launched from Earth at 1 a.u., and the data with the LORRI dust cover in place were acquired at 1.9 a.u., just beyond Mars' orbit at 1.5 a.u. (inner blue dotted lines). The dust cover was ejected near 3.6 a.u., and the data were acquired before and during an encounter with Jupiter. The data considered here were taken between 2007 and 2010 while New Horizons was in cruise phase. The red vectors indicate the relative positions of fields 1–4 compared to the sun and plane of the ecliptic.

brightness of each component, particularly those that appear constant over angular scales similar to the field of view of the instrument.

We isolate $\lambda I_\lambda^{\text{COB}}$ using three basic steps: mask stars near or brighter than the detection threshold to remove the effect of λI_λ^* ; subtract the diffuse components either originating in the instrument or from local astrophysical emission to isolate the

Table 1 | Data sets used in this analysis.

Field number	α (J2000) hh:mm:ss	δ (J2000) hh:mm:ss	ℓ ($^\circ$)	b ($^\circ$)	e_b ($^\circ$)	A_V (mag)
1	13:04:02	23:57:02	345.4147	85.7384	28.2096	0.06
2	10:47:36	-26:46:56	271.4532	28.4141	-31.5843	0.22
3	23:04:27	-7:07:00	66.2722	-57.6861	-1.0847	0.16
4	00:07:14	-1:15:00	98.8079	-62.0328	-1.8651	0.10

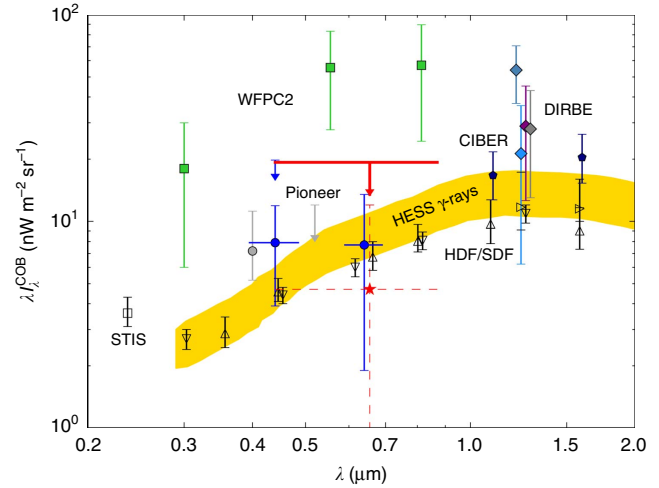


Figure 2 | Measurements of the COB surface brightness. The $\lambda I_\lambda^{\text{COB}}$ determined in this study are shown as both an upper limit (red) and a mean (red star). We also show previous results in the literature, including direct constraints on the COB (filled symbols) and the IGL (open symbols). The plotted LORRI errors are purely statistical and are calculated from the observed variance in the mean of individual 10 s exposures; see Fig. 3 for an assessment of the systematic uncertainties in the measurement. We include the measurements from HST-WFPC2 (ref. 7; green squares), combinations of DIRBE and 2MASS^{10–13} (diamonds; the wavelengths of these measurements have been shifted for clarity), a measurement using the ‘dark cloud’ method⁸ (grey circles), and previous Pioneer 10/11 measurements^{22,23} (blue upper limit leader and circles). The gold region indicates the H.E.S.S. constraints on the extragalactic background light²⁹. We include the background inferred from CIBER⁵ (pentagons). The IGL points are compiled from HST-STIS in the ultraviolet (UV)⁶² (open square), and the Hubble Deep Field⁶³ (downward open triangles) the Subaru Deep Field^{64,65} (upward open triangles and sideways pointing triangles) in the optical/near-IR. Where plotted, horizontal bars indicate the effective wavelength band of the measurement. Our new LORRI value from just 260 s of integration time is consistent with the previous Pioneer values.

diffuse residual component $\lambda I_\lambda^{\text{resid}} = \epsilon \lambda I_\lambda^{\text{COB}}$; and correct the mean residual intensity for the effects of galactic extinction to yield $\lambda I_\lambda^{\text{COB}}$. Averaging over all the fields using inverse noise variance weighting, we determine that $\lambda I_\lambda^{\text{COB}} = 4.7 \pm 7.3 \text{ nW m}^{-2} \text{ sr}^{-1}$, where the uncertainty is purely statistical and is assessed from the scatter in the individual exposures. This gives a 2σ upper limit on the COB brightness of $\lambda I_\lambda^{\text{COB}}(2\sigma) < 19.3 \text{ nW m}^{-2} \text{ sr}^{-1}$. Our measurement and comparisons with previous measurements in the literature are shown in Fig. 2.

This measurement is also subject to various systematic uncertainties associated with the calibration and foreground removal. We carefully assess these errors by probing the allowed variation in each of the models and measurements to derive an overall calibration and systematic uncertainty budget,